PHYSICAL REVIEW B VOLUME 40, NUMBER 12 15 OCTOBER 1989-II

Photoreflectance from GaAs and GaAs/GaAs interfaces

Michael Sydor, James Angelo, and Jerome J. Wilson
Department of Physics, University of Minnesota–Duluth, Duluth, Minnesota 55812

W. C. Mitchel
Materials Laboratory, Air Force Wright Aeronautical Laboratories, Wright-Patterson Air Force Base, Ohio 45433

M. Y. Yen
Systran Corporation, 4126 Linden Avenue, Dayton, Ohio 45432
(Received 29 August 1988; revised manuscript received 12 May 1989)

Photoreflectance from semi-insulating GaAs, and GaAs/GaAs interfaces, is discussed in terms of its behavior with temperature, doping, epilayer thickness, and laser intensity. Semi-insulating substrates show an exciton-related band-edge signal below 200 K and an impurity-related photoreflectance above 400 K. At intermediate temperatures the band-edge signal from thin GaAs epilayers contains a contribution from the epilayer-substrate interface. The interface effect depends on the epilayer's thickness, doping, and carrier mobility. The effect broadens the band-edge photoreflectance by 5–10 meV, and artifically lowers the estimates for the critical-point energy, E_{CP}, obtained through the customary third-derivative functional fit to the data.

INTRODUCTION

Modulated photoreflectance[1–7] (PR) is a common, nondestructive technique for optical measurement of the band-gap energies, doping concentrations, and alloy composition in GaAs and $\mathrm{Al}_x\mathrm{Ga}_{1-x}\mathrm{As}$.[8–10] The technique could have application as an optical diagnostic tool for the determination of sample quality in molecular-beam epitaxy (MBE). However, before such applications can be made, much remains to be done on the fundamental properties of PR, especially its properties from interfaces, at elevated temperatures.

Ordinarily, in most PR experiments, the critical-point energy, E_{CP}, is determined by fitting the shape of the signal at the band edge with the third-derivative functional form (TDFF) for low electric fields.[6,8] The precise location of the critical-point energies and their subsequent use in determination of carrier concentrations,[8] alloy composition,[10] etc., depends on rather precise theoretical fits to the PR data. The theory, in turn, relies on assumption of specific physical processes.[6] The main process is the interaction of electrons with the electric field in the space-charge region (SCR). This process dominates the PR above the band-gap energies and is prominent in doped samples. The PR below the band gap includes exciton effects and involves a superposition of processes. The complexity of the band-edge PR is described by Peters *et al.*[8] These authors, in their analysis of PR data, invoke room-temperature excitonic nature of PR response to account for the fact that the critical-point energy they obtain from TDFF falls below the nominal band-gap energy for GaAs. Peters *et al.*,[8] using very accurate PR measurements and TDFF analysis, observed shifts in E_{CP} with doping and used these shifts in determination of the carrier concentrations for ion-implanted samples. Their method was accurate for the ion-implanted samples, but was less fruitful for doped MBE samples, where the calculated shifts in E_{CP} fell below the ion-implanted values. The authors resolved this difficulty by considering the differences between the dopant distribution in the ion-implanted and the MBE-doped samples.

On the other hand, Bottka *et al.*[9] chose to circumvent the complexities of band-edge PR analysis by considering instead, properties of the oscillatory PR above the band edge. They developed a relationship between the carrier concentrations, the built-in surface potential V_b, and the energy period of the PR oscillations. Subsequently, they used the oscillations in the determination of doping concentrations for samples grown by chemical vapor deposition (CVD).

We report here on several measurements which were devised to isolate the origin of the band-edge PR in the semi-insulating substrates and investigate the nature of PR from the epilayer-substrate interfaces. We will discuss our results in the light of known PR mechanisms,[6,8,9,11] and address the merits of the above two techniques for the optical determination of carrier concentrations.[8,9] In particular, we will show that interface effects detected here can distort the band-edge PR, and introduce errors in the commonly accepted TDFF analysis of the data. Our results will also show that the PR oscillations method[9] provides accurate determinations of the band-gap energy for MBE samples, independent of the shape of the band-edge PR.

In this paper, we will have two distinct regions of interest; the PR signal just below the band-gap energy and the oscillatory PR above the band gap. We will use the term band-edge PR loosely to refer to the signal in the 0–10-meV region below the nominal band-gap energy. This region will include the excitonic PR discussed by Peters *et al.*[8] and the interface PR which we detected in our experiments.

 ©1989 The American Physical Society

THEORETICAL BACKGROUND

We present a brief outline of the theory and terminology needed in the analysis and discussion of our data.

The PR signals for GaAs samples can be classified into two categories according to the magnitude of the surface electric field E_s. The first category is the high-field condition, where the surface field is large. This is usually the case for doped samples. The second category is the low-field condition, which usually occurs for undoped samples. Aspnes[6] showed that the PR signal is in the low-field limit when

$$\hbar\Omega < \Gamma/3 \ . \qquad (1)$$

$\hbar\Omega$ is a characteristic energy associated with the critical point. It is related to E_s by

$$\hbar\Omega = (e^2 E_s^2 \hbar^2 / 8\mu)^{1/3} \ , \qquad (2)$$

where μ is in interband reduced mass and Γ is a broadening parameter for the critical-point energy $E_{\rm CP}$. Aspnes also derived a quick rule of thumb, if the PR signal is such that

$$\Delta R/R < 10^{-4} \ , \qquad (3)$$

then the signal is in the low-field limit. In the low-field limit, the line shape for PR is given by[6]

$$\Delta R/R = \mathrm{Re}[Ce^{i\theta}(\hbar\omega - E_{\rm CP} + i\Gamma)^{-n}] \ , \qquad (4)$$

where $\hbar\omega$ is the energy of the probe beam and C and θ are an amplitude and phase factor that vary slowly with $\hbar\omega$. n refers to the type of critical point in question; $n=2$, 2.5, and 3 for an exciton, a three-dimensional band-to-band transition, and a two-dimensional band-to-band transition, respectively. This relationship is frequently used to fit PR data for undoped and doped samples which meet the low-field criteria.[8]

In the high-field limit, the PR signal is proportional to the product of Airy functions and their derivatives. These take the asymptotic form[7]

$$\Delta R/R \propto \cos\{\tfrac{2}{3}[(\hbar\omega - E_{\rm CP})/\hbar\Omega]^{3/2} + \pi(d-1)/4\} \ , \qquad (5)$$

where d is the dimensionality of the critical point. For GaAs, with a direct transition, $d=3$. This line shape has an oscillatory nature where the oscillations are termed Franz-Keldysh oscillations (FKO). Neglecting the amplitude factor in Eq. (5), the position of the FKO peaks is approximated by [12]

$$(\hbar\omega)_j = \hbar\Omega(F_j) + E_g, \quad j=1,2,3,\ldots \ , \qquad (6a)$$

where

$$F_j = [3\pi(j-\tfrac{1}{2})/2]^{2/3} \ . \qquad (6b)$$

As indicated by Eq.(6), a plot of $(\hbar\omega)_j$ versus F_j is a straight line, with slope $\hbar\Omega$ and intercept E_g. This plot uses the FKO extrema marked $j=1$, 2, etc. in sequence, beginning with the first pronounced extremum following the PR signal at the band gap (see Fig. 9). $\hbar\Omega$ is related to E_s by Eq. (2). By assuming a reduced mass,[12] $\mu = 0.057 m_e$, the surface electric field can be determined. Bottka *et al.*[9] have shown that the field so determined is related to the carrier concentration N and the built-in potential V_b by the generalized Schottky equation

$$E_s = [2eN(V_b - V_p - kT/e)/\kappa\epsilon]^{1/2} \ , \qquad (7)$$

where V_p is the quasiequilibrium photovoltage of the laser, kT/e is a thermal term, and $\kappa\epsilon$ is the dielectric constant times the permittivity of free space. Because of pinning at the surface, $V_b = 0.73$ V (Ref. 13) and $\kappa = 13.18$ for GaAs.[9] V_p was determined from Eq. (7) using calibrated samples where N was known. Bottka *et al.*[9,12] used the slopes given by Eq. (6) to determine the carrier concentrations in Si-doped samples of GaAs grown by CVD.

The slope of the lines given by Eq. (6) appears to depend only on the carrier concentrations, independent of the laser energy and intensity, and sample preparation. For instance, CVD samples fall along the same straight lines as the MBE samples, when they have the same Hall carrier concentrations.[14] Usually, the intercept E_g obtained from Eq. (6) falls close to the critical-point energy $E_{\rm CP}$ calculated by TDFF from Eq. (4), except for thin MBE samples where the band-edge PR is distorted by the interface effects. We will show that E_g given by Eq. (6) is insensitive to the shape of the band-edge PR and that it follows, with temperature, the relationship due to Thurmond:[15]

$$E_g = 1.519 - 5.405 \times 10^{-4}[T^2/(T + 204\ \mathrm{K})] \ , \qquad (8)$$

where T is the absolute temperature in degrees Kelvin and E_g is in eV.

EXPERIMENT

We used a standard arrangement of photoreflectance apparatus[5] to measure the PR from undoped and lightly doped GaAs, grown by MBE on semi-insulating substrates. Signal modulation was achieved with a 5-mW HeNe laser beam chopped at 400 Hz. The intensity of the modulation beam ranged from 10–100 mW/cm^2. As a check on the laser excitation effects, some data was repeated using a 7-mW HeCd laser. The shape of the PR remained the same. Usually a 100-W tungsten-halogen lamp coupled to a 0.25-m monochromator was used to scan the samples for photoreflectance $\Delta R/R$ over a wavelength range of 700–1000 nm. The samples were mounted in a rotatable dewar, which allowed us to take data at reflectance angles ranging from 15° to 65°, and temperatures ranging from 77 to 600 K. Narrow-band-pass filters were used in front of the probe beam detector to check for room-temperature photoluminescence.[16] For the sake of comparison, and instrument checkout, several CVD epitaxial samples were examined. In particular, a sample, accompanied with PR data, was provided to us by Gaskill[9] (U.S. Naval Research Laboratories, Washington, D.C.). The sample was used as a comparative standard to test the performance of our equipment. The PR data for the sample was invariably the same in all experimental setups.

Because we suspected that the interface effects which

we observed could be associated with strain,[12] we took Raman spectra for several representative samples. The Raman spectra were the same to within 0.2 wave numbers for all samples. Two thin samples, with pronounced interface effects, were also examined for changes in PR with laser chopping frequency. By varying the chopping frequency from 5 to 3500 Hz, no significant long-lifetime effects were observed.

RESULTS

We present the data in three sections: Semi-insulating substrates; thick MBE material, and interface effects. In each section we will examine the effects on PR due to field modulation,[6,9,12] exciton effects,[17,11] and effects from impurities or traps.[12,18,19]

Semi-insulating substrates

Bulk material PR and TDFF

Figures 1 and 2 show the PR for a semi-insulating substrate and a doped bulk sample. The semi-insulating material, Fig. 1, provides a low-PR signal at and just below the nominal band-gap energy of 1.424 eV. This PR is typical of the semi-insulating samples. It shows a modulation signal of the form given by Eq. (4), as expected for the low-field conditions in semi-insulating material. We notice that the energy of the PR signal in Fig. 1 appears low, possibly due to the exciton effects mentioned by Peters *et al.*[8]

The effect of doping on the bulk material can be seen in Fig. 2. The shape of the PR from the doped sample is similar to the PR in Fig. 1, except for a moderate deepening of the PR minimum above the band gap, and an inflection in the signal at E_g. The sample had 1.6×10^{15} cm^{-3} In and 1.2×10^{15} cm^{-3} Si concentrations. A

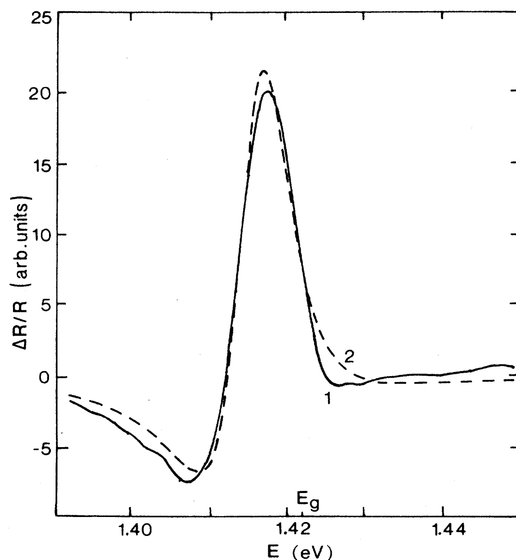

FIG. 1. Curve 1, PR from semi-insulating substrate. Curve 2, TDFF fit with exciton critical point $n=2$, and $E_{CP}=1.416$ eV.

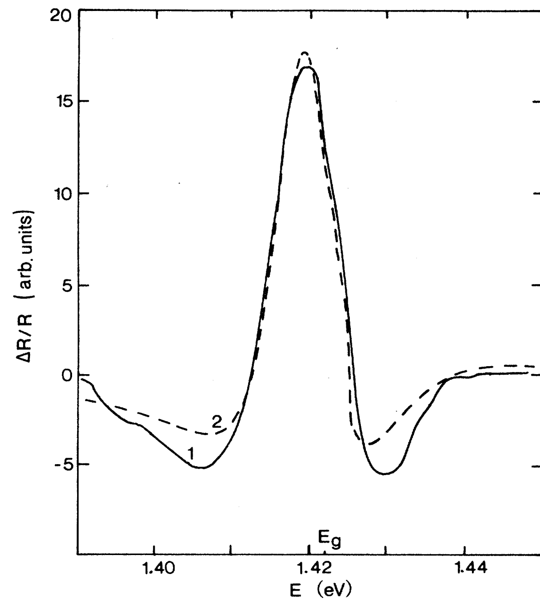

FIG. 2. Curve 1, PR from a doped bulk sample (1.6×10^{15} cm^{-3} In, 1.2×10^{15} cm^{-3} Si). Curve 2, the functional fit consists of a sum, an exciton critical point used in Fig. 1, and a three-dimensional critical point with $n=2.5$ and $E_{CP}=1.421$ eV.

1.2×10^{15} cm^{-3} Si doping in MBE or CVD samples produces large band-edge PR accompanied by pronounced FKO. The doped bulk sample shows none of these effects. However, the inflection in PR in Fig. 2 suggests a superposition of two processes. It appears that the effect of doping produces an additional signal on top of the band-edge PR whose origin may be different from the carrier-field interaction.[6] Thus, a question arises regarding the origin of the band-edge PR in the semi-insulating material. Is it associated with excitons[8,9,11,17] or impurities? Impurity effects, occurring 15–25 meV below E_g, are often reported in the PR spectra but are generally dismissed from lack of data, as nuisance effects.

The TDFF for the two bulk samples are shown in Figs. 1 and 2. Considering all possible forms given by Eq. (4), the best TDFF for the semi-insulating sample in Fig. 1 was obtained by using an exciton critical point with $n=2$, and E_{CP} at 1.416 eV. The doped sample in Fig. 2 could not be fitted with a single function of the form given by Eq. (4). However, a sum of an exciton and an additional three-dimensional band-to-band transition with $n=2.5$ and E_{CP} at 1.421 eV, provided a reasonable fit to the data, as shown in Fig. 2. The TDFF for the semi-insulating sample was in keeping with the results of Peters *et al.*,[8] except, in our case, the exciton critical-point energy was low by ~4 meV. It would appear that the signal we observe may be due, at least in part, to impurities.

Effects of coatings on PR from substrates

In an attempt to separate out the contributions to PR due to excitons,[8,11,17] electron transitions, and impurities,

we decided to compare the PR data from bare and epi-coated semi-insulating substrates over a wide range of temperatures. The reasoning behind this procedure was the fact that exciton effects should change with an increase in surface potential V_b, and quench with an increase in temperature.[11,17] A thin $Al_xGa_{1-x}As$ coating would be transparent to the probe beam, but would absorb laser light. The coating should produce a change in V_b at the substrate surface but should confine laser-induced change in light absorption[20] largely within the $Al_xGa_{1-x}As$ coating. However, modulation caused by laser-injected carriers[8] should still be effective through the thin $Al_xGa_{1-x}As$ coatings. On the other hand, a 1–4-μm epicoating of undoped GaAs should match the substrate band-gap energy and remove field-modulation effects from the substrate surface.

We consider first, the effects of changing V_b at the substrate surface by coating the substrate with a 0.15-μm MBE layer of $Al_{0.3}Ga_{0.7}As$. As expected,[6,9,11] the results showed large oscillatory PR above the band-gap energy. However, the signal at the band edge diminished considerably from its amplitude in the bare substrate, as shown in Fig. 3. (The PR in Fig. 3 is due to GaAs. $Al_xGa_{1-x}As$ PR appears well above the energy range shown in Fig. 3.) The separation and the amplitude of the oscillatory peaks in Fig. 3 indicate[11] that the electric field and the modulation field within the coated substrate are comparable with the fields observed in bare undoped and lightly doped MBE samples.[14] Such fields could be sufficient to produce exciton modulation.[9,11,17] Thus, if the band-edge PR in the uncoated semi-insulating material was largely due to excitons, field effects produced by the $Al_xGa_{1-x}As$ coating could in principle account for the observed decrease in the band edge signal in Fig. 3. The remnant signal below the band gap could thus be attributed to the absorption edge PR and excitons from beyond the effective SCR produced by the coating. To test this assumption, we consider the behavior of PR with temperature.

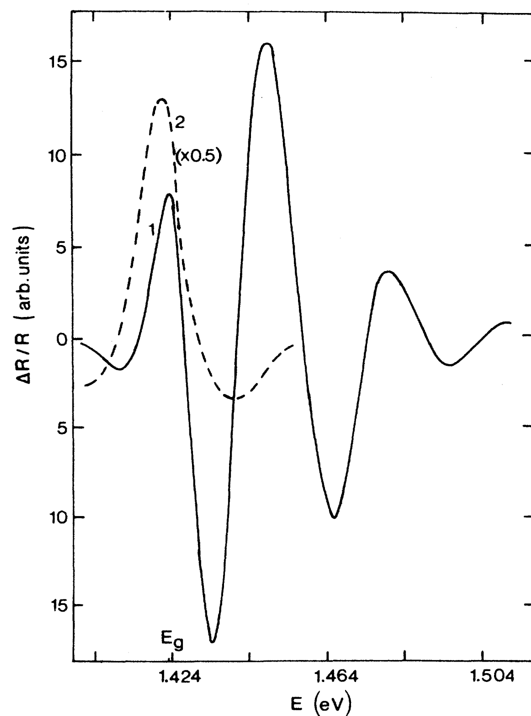

FIG. 3. Curve 1, PR from a semi-insulating substrate covered with 0.15-μm layer of $Al_{0.3}Ga_{0.7}As$ (MBE). Notice the pronounced FKO beyond 1.424 eV. Curve 2 shows the PR from the bare semi-insulating substrate. The amplitude of curve 2 has been reduced ($\times 0.5$).

Temperature dependence of PR in coated substrates

Temperature dependence of PR in the $Al_xGa_{1-x}As$-coated substrate indicates that the band-edge signal has a different origin from the free excitons beyond the SCR. As the temperature of the coated substrate increased to 375 K, Fig. 4 shows that band-edge PR in the coated substrate increased substantially, relative to the oscillatory PR. This increase with temperature is contrary to the behavior expected from the carrier dependent PR,[6] and contrary to the temperature dependence expected from free excitons.

As the temperature of the sample increased beyond 400 K, Fig. 5 shows that the entire PR for the $Al_xGa_{1-x}As$-coated substrate changed abruptly, simulating the effect of an increased carrier concentration.[14] The resulting band-edge signal increased slightly, but it broadened substantially, while the FKO diminished and spread out. Furthermore, the FKO in this broadened signal fell along

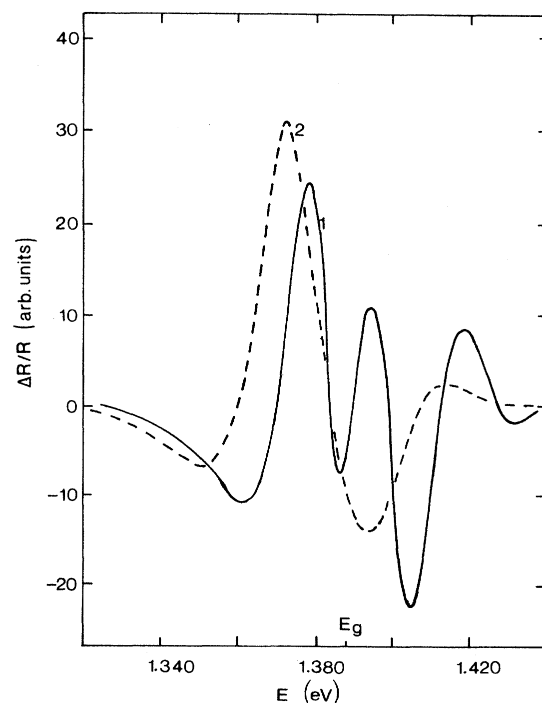

FIG. 4. PR at 375 K. Curve 1, $Al_{0.3}Ga_{0.7}As$-coated substrate. Curve 2, bare semi-insulating substrate after the $Al_xGa_{1-x}As$ has been etched off.

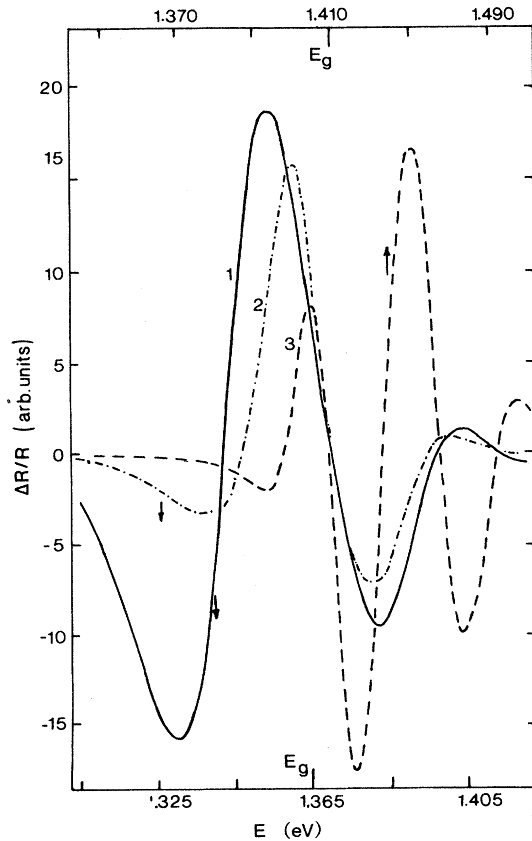

FIG. 5. PR at 415 K. Curve 1, PR for $Al_xGa_{1-x}As$-covered substrate broadens abruptly. Curve 2, the bare semi-insulating substrate shows well-developed FKO.

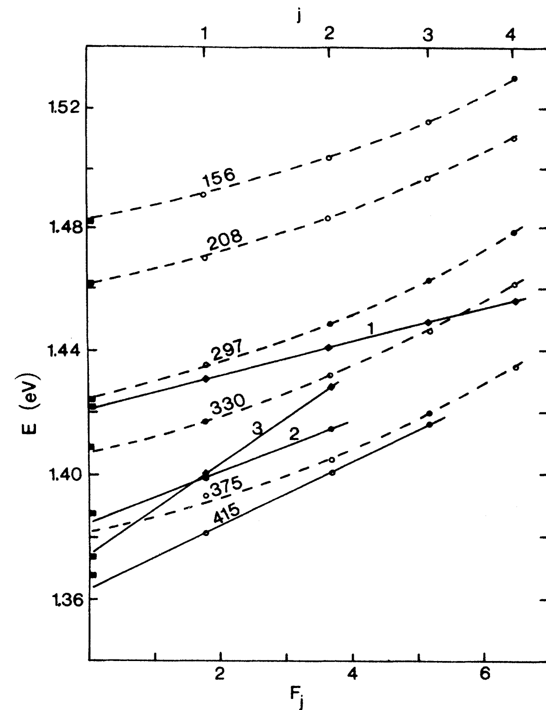

FIG. 6. Dashed lines—plot of PR oscillation peaks for the $Al_xGa_{1-x}As$-coated semi-insulating material vs number F_j [see Eq. (6)]. Temperatures of the coated substrate are indicated on the graph. Above ~400 K the semi-insulating properties of the substrate change, and the plot for the coated substrate at 415 K is a straight line, typical of undoped MBE material. Curve 1, FKO plot for Si-doped (10^{15} cm^{-3}) MBE sample. Curve 2 shows the FKO plot for the bare substrate at 375 K. Curve 3, FKO plot for semi-insulating material at 400 K (different source than the bare substrate from curve 2). (■), the E_g values according to Thurmond (Ref. 15).

straight-line plots according to Eq. (6), a result typical of the MBE samples. This is shown by the solid straight line at 415 K in Fig. 6. This abrupt change in the nature of the FKO indicates that the character of the substrate has changed at the elevated temperature, from semi-insulating properties to properties of undoped MBE material. We note here, in reference to a following discussion, that the FKO plot for this sample provides a good estimate of E_g at 415 K, even though its band-edge PR has become quite distorted.

Decrease in temperature provides another insight into the nature of PR from the semi-insulating material. The amplitude of the FKO in the coated substrate diminishes at lower temperatures, but their spacing remains relatively unchanged. However, the band-edge PR drops off rapidly at lower temperatures, and disappears altogether below 150 K, leaving behind a low-absorption-edge PR, shown in Fig. 7. This situation is quite different for the bare substrate.

Temperature effects and exciton related PR in bare substrates

Change in temperature produced significant changes in the PR from the bare substrate. As the temperature increased, the PR above the band gap began to display distinct PR oscillations, as was shown in Figs. 4 and 5. The onset of FKO in the bare substrate confirms that the flat-band condition in the semi-insulating substrate changed at higher temperatures. However, the decrease in temperature showed a substantial difference between the bare and the coated substrate. In bare substrates, the band-edge PR still diminished with temperature as it did in the $Al_xGa_{1-x}As$-coated substrate, but at temperatures below 200 K, a new narrow PR signal emerged from the bare substrate, Fig. 7. The energy of the new signal coincided with the free exciton energy. This narrow PR is usually associated with thick, undoped MBE samples. It can be seen, from curves 3 and 4 in Fig. 8, that the new signal has the same temperature dependence as the band-edge PR from undoped MBE samples. It is believed that the narrow PR is due to free excitons[5,8] and that the modulation mechanism for the excitons in the semi-insulating material, where fields are low, comes from laser-induced changes in the light absorption for GaAs at exciton energies.[20–22] Existence of such a modulation mechanism is

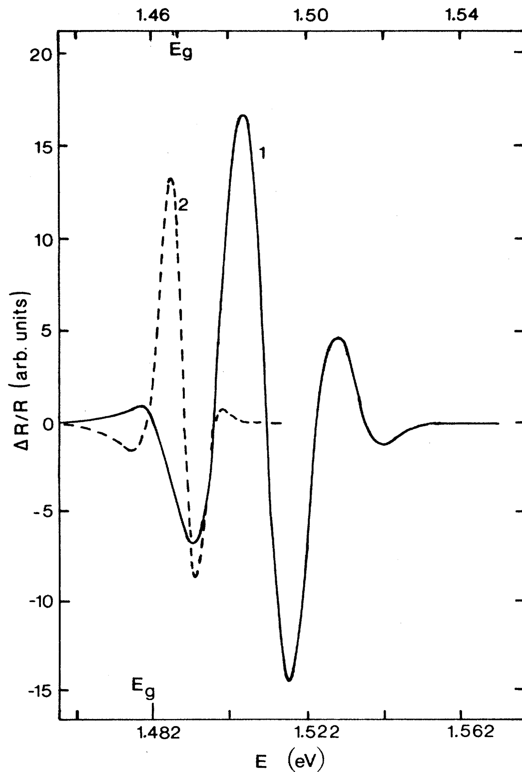

FIG. 7. Curve 1, PR for the $Al_xGa_{1-x}As$-coated substrate at 156 K shows the disappearance of the impurity PR below the band edge. Curve 2, exciton-related PR appearing in the bare semi-insulating substrate at 200 K, after the $Al_xGa_{1-x}As$ has been etched off.

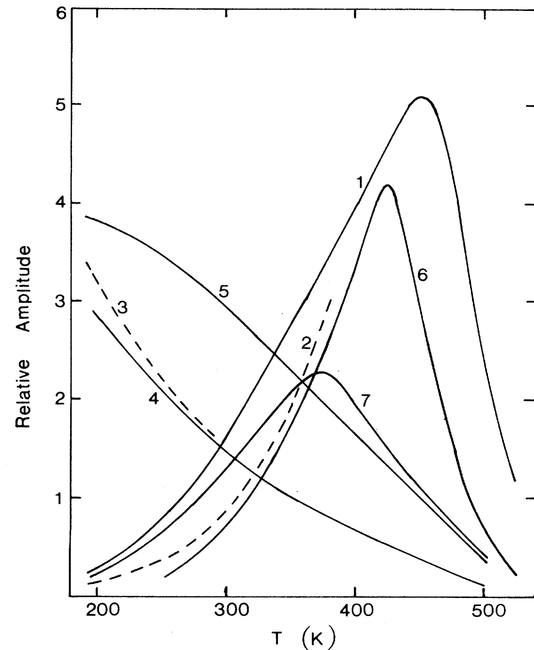

FIG. 8. Temperature dependence of various PR signals. Curve 1, band-edge PR from a semi-insulating substrate. Curve 2, band-edge PR from an $Al_xGa_{1-x}As$-coated semi-insulating substrate. Curve 3, band-edge PR at low temperature from a bare semi-insulating substrate after the $Al_xGa_{1-x}As$ has been etched off. Curve 4, band-edge PR from a thick, undoped MBE sample. Curve 5, band-edge PR from Si-doped MBE sample. Curve 6, temperature dependence for interface PR, structure A, for undoped GaAs on semi-insulating substrate. Curve 7, temperature dependence of structure A for doped GaAs on semi-insulating substrate.

supported by the fact that the excitonic PR is absent in the $Al_xGa_{1-x}As$ coated substrate at low temperatures. Its absence is probably due to lack of modulation. Laser modulation of the electric field through carrier injection was sufficient to produce the FKO in the coated substrate, but the fields were insufficient to produce exciton quenching effects.[11] Furthermore, the laser-generated carrier densities originating in the coating were insufficient to modulate the refractive index of the substrate at the exciton energy.[21] On the other hand, direct injection of laser generated carriers at the bare GaAs surface may produce sufficient changes in absorption[21,22] to give rise to the observed narrow excitonic PR.

Mechanism for band-edge PR from traps or impurities

The general freeze-out of the band-edge PR and its sharp onset with temperature increase, curves 1 and 2 of Fig. 8, suggests that the band-edge signal from semi-insulating substrates at room temperature comes mainly from inherent traps or impurities or possibly bound excitons. The temperature dependence shown in Fig. 8 was nearly the same for semi-insulating samples from three different sources. The modulation mechanism responsible for this PR appears to be due to a thermal emptying of the traps, or a thermal dissociation, and a momentary refilling of the traps by the laser-injected carriers.

This proposed mechanism is also needed in explanation of the band-edge PR from substrate surfaces buried by 1–4-μm-thick GaAs epilayers. Undoped GaAs epilayers isolate the substrate surface from field modulation effects, yet, the trap or impurity related PR, which appears as an interface effect in the GaAs coated substrates, is quite evident when one compares the PR in Figs. 9 and 10. The origin of the band-edge PR structure A, Fig. 10, will be traced directly to the epilayer-substrate interface through use of interference measurements which will be discussed in detail in the section entitled, interface effects.

Determination of E_g from FKO plots

Before we leave this section we wish to show that the oscillatory PR and E_g in the $Al_xGa_{1-x}As$-coated substrates follows the expected[15] temperature behavior for the PR from GaAs and that the coating mainly serves the purpose of imposing a change in surface potential V_b. We also want to consider results which support the FKO

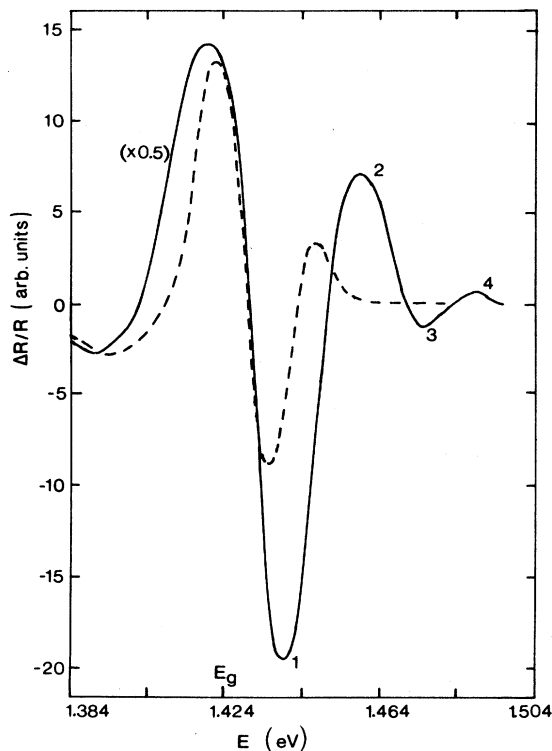

FIG. 9. Examples of PR from thick MBE samples. Dashed line, undoped 8.6-μm sample. Solid line, the PR from 1×10^{15} cm^{-3} Si-doped 4.4-μm MBE sample. The amplitude of the doped sample has been reduced ($\times0.5$). Labels 1, 2, 3, and 4 refer to the successive j values for the FKO peaks in Eq. (6).

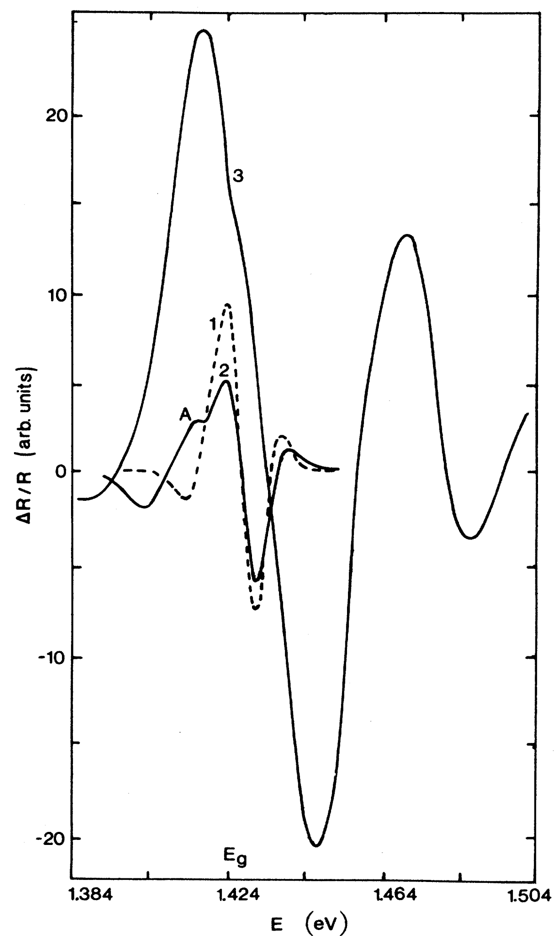

FIG. 10. Indications of presence of the interface PR in thin MBE samples. Curve 1, PR from undoped 4.2-μm MBE sample shows no interface effect. Curve 2, PR from 2.3-μm undoped MBE GaAs shows a pronounced interface PR, labeled as structure A. Curve 3, PR from a 2.4-μm Si-doped (8×10^{15} cm^{-3}) MBE sample. For the doped sample, the interface effect dominates the PR at the band edge, and only an inflection at E_g signifies presence of two PR mechanisms.

method for measurement of the carrier concentrations.[9]

We mentioned that the plot of FKO according to Eq. (6) can be used in the determination of carrier concentrations, and in the evaluation of E_g. Figure 6 shows the plots for a variety of samples. Curve 1 shows a 10^{15} cm^{-3} Si-doped MBE sample. Its FKO lie along a straight line, as expected from Eqs. (6) and (7) with the intercept E_g at 1.422 eV. Similarly, curve 2 of Fig. 6 shows the results for the bare semi-insulating substrate at 375 K, when the FKO begin to set in. Again, the intercept for this sample lies close to the E_g expected at this temperature.[15] Curve 3 shows a substrate of different origin at 400 K with similar results for the E_g. Curve 3 has a steeper slope than curve 2, indicating a higher level of unintentional impurities in the second substrate.

For the $Al_xGa_{1-x}As$-coated substrate, the FKO plots are shown in Fig. 6 by the broken lines with sample temperatures marked on each line. The FKO are close together as expected for the low carrier concentration.[9,11,14] However, the peaks do not lie along straight lines for the coated semi-insulating material, as they would for MBE samples when Eqs. (6) and (7) hold. We note that the separation of FKO for the coated sample remains nearly fixed with temperature, as indicated by the parallel dashed lines in Fig. 6. This result is expected, since the electric field in the coated substrate is determined by the $Al_xGa_{1-x}As$ band gap, the unintentional impurities in the $Al_xGa_{1-x}As$, and the flat-band, semi-insulating nature of the substrate, a condition which did not change until $\sim$400 K. Surprisingly, the extension of the broken lines in Fig. 6 to the intercept with the energy axis produces E_g values which, as seen in Fig. 6, are in good agreement with those predicted for GaAs by Thurmond.[15]

In summary, we note that the intercepts shown in Fig. 6 produced the expected E_g in all samples, coated and bare, even when the shapes of the PR near the band edge were a different as those shown in Figs. 4 and 5. These results show that the field effects in the FKO region are described well by Eqs. (5), (6), and (7), and that the FKO method[9] provides a reliable determination of E_g, indepen-

dent of the shape of the band-edge PR. Furthermore, doping concentrations determined from the slopes in Fig. 6, appear insensitive to small changes in sample temperature.

Thick MBE material

Thick, undoped MBE material has a narrow PR signature, as shown by examples in Figs. 9 and 10. Unlike the bulk material, the PR from the thick MBE samples has a monotonic decrease with temperature, as shown by curves 4 and 5 in Fig. 8. The shape of the PR signal sharpens at lower temperatures, but its general character remains relatively unchanged over the temperature range discussed here. In comparison with the PR from the semi-insulation substrates, the undoped MBE material does not show a flat-band condition at any temperature. Its PR always shows a full oscillation above the band gap, with a distinct peak corresponding to the second FKO, as shown in Fig. 9. At room temperature the separation of the FKO peaks for the undoped MBE samples was correlated with the unintentional impurity concentrations.[14]

Light Si doping of the MBE samples invariably broadens the PR below the band gap and enhances the FKO peaks, as shown in Fig. 9. In MBE samples the PR above the band gap behaves according to the theory.[6,9,11] However, as was the case in the semi-insulating material, the origin of the PR below the band edge appears less certain,[8] especially for the undoped material. The sharp rise in the band-edge PR for undoped samples at low temperatures, in comparison with the band-edge PR for the doped samples, Fig. 8, suggests the band-edge PR in undoped MBE samples comes from a combination of signals due to unintentional impurities and excitons. Existence of excitonic PR below the band gap is well known.[8,9,11] However, in the case of low fields, the nature of the excitonic modulation mechanism is uncertain. It has been established that the field-modulated excitonic PR in doped samples comes from fluctuation of the SCR, exciton quenching, and the associated interference effects,[9,11,17] but for the flat-band conditions[8] and the relatively low fields in undoped MBE material, fields due to V_b and V_p appear insufficient to modulate exciton-related reflectance in the semi-insulating substrates and the undoped MBE material. The results of interference measurements, treated in the following section, will show that the band-edge PR in these materials comes from the surface region of the sample, a region which is on the same order of thickness as the laser-light absorption region.

Interface effects

Distortions in the band-edge PR

A superposition of effects, contributing to the band-edge PR, is often manifested by an inflection, or a kink, in the PR signal. In the thin MBE samples, interface effects are visible through the epilayer and distort the band-edge PR. Such distortions are evident in some samples, as shown by the two examples in Fig. 10. Here, the PR from the interface is labeled as structure A and will be referred to as such in the remaining text. We notice, that for undoped MBE samples, the distortion appears on the low-energy side of the band-edge PR. In doped samples, the interface effect is dominant, and its presence is signified only by an inflection at E_g. In higher-doped samples, presence of the interface effect may be completely disguised. However, the effect generally broadens the band-edge PR by 5–10 meV and lowers the TDFF estimates of E_g by 0–5 meV, depending on the thickness of the MBE epilayer. The results in Fig. 1 showed a 4-meV shift in the excitonic TDFF applied to the data for a bare semi-insulating substrate. In epicoated substrates this shift may be lower. At elevated temperatures the interface effect is visible even through epilayers thicker than 4 μm. In such instances, it only drags out the low-energy tail of the band-edge PR.

Dependence of structure A on epilayer thickness

To establish the fact that structure A comes from the epilayer-substrate interface, we examine its dependence on epilayer thickness. Figure 11 shows that the amplitude of structure A drops off according to the exponential absorption law, with a coefficient $\alpha=3.47\times10^3$ cm^{-1}. This value for the absorption coefficient is comparable with the value quoted for GaAs by Blakemore.[20]

Further verification of the dependence of structure A on the epilayer thickness was obtained from interference measurements by varying the reflectance angle θ relative to the normal in air. Figure 12 shows the PR for a lightly doped, 1.8-μm-thick epilayer at $\theta=48°$, when structure A attains a maximum amplitude. If we consider that the light reflected at the front surface of the epilayer is independent of the sample thickness, then the change in structure A, with θ, can be explained in terms of the interference of light reflected at the front surface of the epilayer with the light reflected at the substrate surface. For an epilayer thickness t, the change in the optical path Δ is

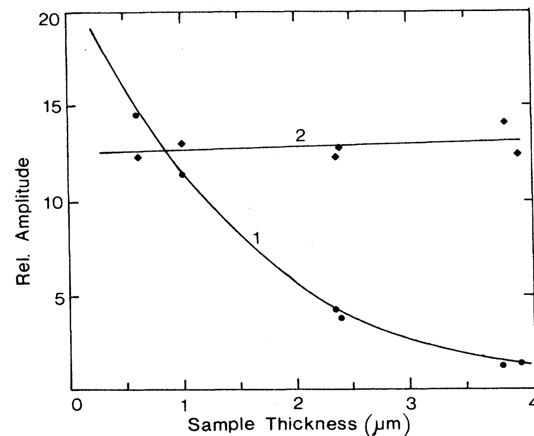

FIG. 11. ●, the amplitude of the interface PR structure A as a function of undoped epilayer thickness. The solid line shows an exponential absorption with $\alpha=3.47\times10^3$ cm^{-1}. Curve 2 shows that the band-edge PR from the space-charge region is independent of the sample thickness.

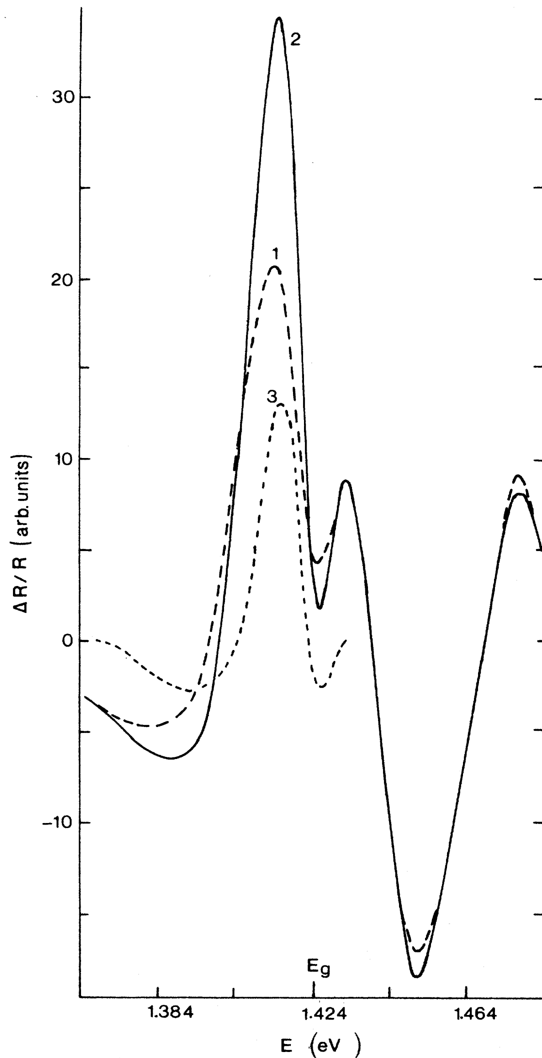

FIG. 12. Superposition of PR from a Si-doped 1.8-μm epilayer as a function of the reflectance angle. Curve 1, PR at $\theta=20°$. Curve 2, PR when structure A is at its maximum at $\theta=48°$. Curve 3, difference in PR between the two cases.

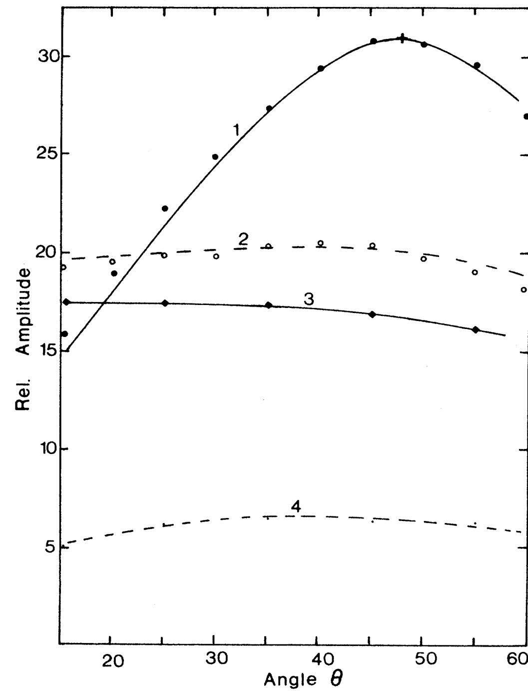

FIG. 13. Curve 1, amplitude of structure A for a 1.8-μm Si-doped (8×10^{15} cm^{-3}) MBE sample, as a function of the reflectance angle θ. Curve 1, the solid line shows the relationship expected from the central spot of thin-film interference pattern. Curve 2, angular dependence of the FKO. Curve 3, angular dependence of the band-edge PR from thick MBE samples. Curve 4, angular dependence of the band-edge PR from $Al_xGa_{1-x}As$-covered substrate.

given by

$$\Delta=2t[(n^2-\sin^2\theta_1)^{1/2}-(n^2-\sin^2\theta_2)^{1/2}] ,$$

where the index of refraction n was taken as 3.6, at wavelength $\lambda=878.4$ nm. The amplitude of the interference signal relative to its maximum at $\theta=48°$, should follow a relationship proportional to $\cos\delta$, where $\delta=2\pi(\Delta_{48°})/\lambda$, and $\Delta_{48°}$ is measured from $\theta=48°$. The amplitude of structure A follows this relationship quite well, as can be seen in Fig. 13. The results shown in Figs. 12 and 13 also show that the PR signals associated with the sample surface region are nearly independent of θ.

Behavior of structure A with temperature

To examine further the identity of structure A, we consider its dependence on temperature. However, care must be taken to account for all temperature effects. The change in sample temperature produces an appreciable change in Δ because of the shift in the band-gap energy with temperature.[23] As seen from curve 6 of Fig. 8, the amplitude of structure A increases nearly tenfold with a temperature increase from 300 to 400 K. This increase in amplitude is much larger than any change attributable to interference. Actually, curves 6 and 7 in Fig. 8 have been already corrected for the temperature effects on Δ. Thermal expansion has been ignored.[23]

At lower temperatures structure A fades out just like the band-edge PR in the semi-insulating substrates. Figure 14 shows how it becomes obscured in a doped MBE sample at 230 K. The general behavior of structure A with energy, sample thickness, and temperature shows that its origin is the same as the trap-related or impurity PR from semi-insulating substrate surfaces.

Dependence of structure A on laser intensity and epilayer doping

Even through the origin of structure A appears to be the same as the trap or impurity-related PR from the substrates, there are distinct differences between the two signals. Structure A shows some additional effects, which

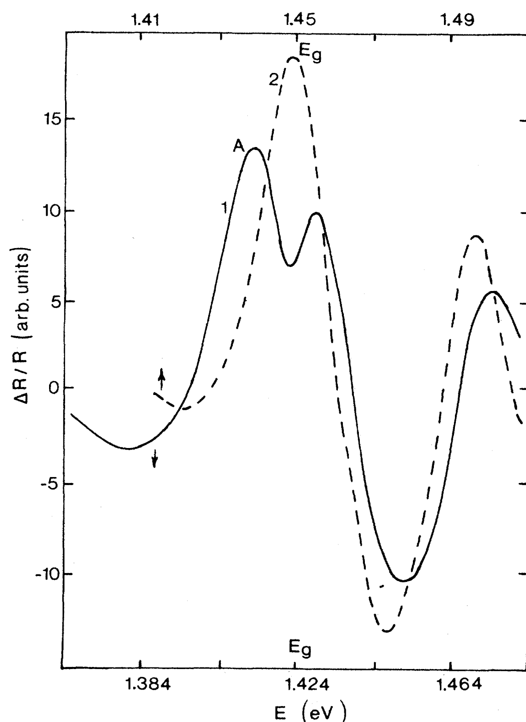

FIG. 14. Decrease with temperature of structure A in a 1.8-μm-thick doped MBE sample. Curve 1, 295 K. Curve 2, 238 K. Structure A disappears altogether at ~ 150 K, see curves 1, 6, and 7 of Fig. 8.

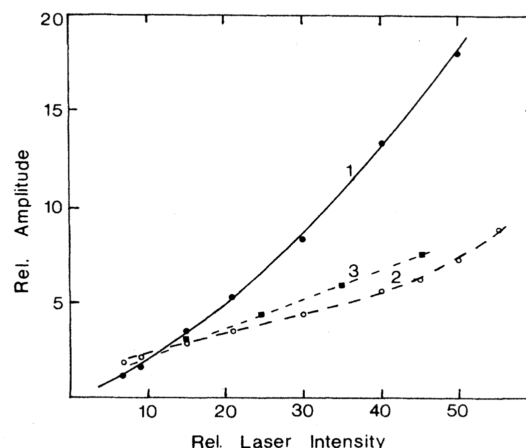

FIG. 15 Curve 1, amplitude of structure A as a function of laser intensity for an undoped epilayer-substrate interface. Curve 2, laser-intensity dependence of the band-edge PR for thick, doped samples. Curve 3, intensity dependence for PR from a semi-insulating substrate.

can be attributed to the properties of the MBE epilayer, and which can shed some light on the nature of the mechanism for the impurity PR. We summarize these additional results as follows.

(1) At room temperature, structure A increases with the epilayer doping.

(2) For fixed doping of $\sim 10^{16}$ cm^{-3}, structure A increases with the Hall mobility.

(3) For undoped MBE epilayers, structure A increases more rapidly with laser intensity than the band-edge PR from the substrates, or the band-edge PR from the thick, doped MBE samples, as shown in Fig. 15.

(4) The energy location of structure A follows E_g as shown in Fig. 16, independent of the epilayer doping. However the amplitude of structure A peaks at a much lower temperature for the doped epilayers. This is shown by curves 6 and 7 in Fig. 8.

DISCUSSION

The residual shape of structure A can be estimated from the difference in PR at the two reflectance angles shown in Fig. 12. By using the residual signal in Fig. 12 and by extrapolating the thermal freeze out of structure A below 150 K, we can say that the traps or impurities are distributed in an 8–13-meV range below E_g.

Results from interference measurements, Fig. 13, show that the band-edge PR in the $Al_xGa_{1-x}As$-coated substrate comes from the substrate surface. This result, coupled with the fact that the band-edge PR was reduced so effectively by the coating, Fig. 3, indicates that the impurity or trap-related PR is a substrate surface phenomenon. If the traps or impurities were distributed throughout the substrate, they would produce an effective population depth, which would exhibit an interference effect with the change in reflectance angle. Interference measurements indicate that the impurity PR for the $Al_xGa_{1-x}As$-coated substrate and for the bare substrate originated at the substrate surface.

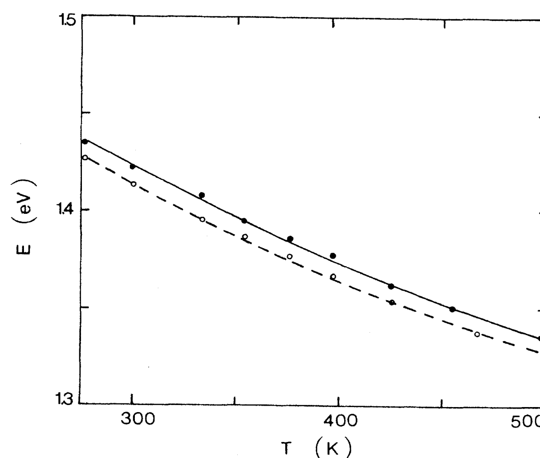

FIG. 16. ○, energy of PR structure A relative to E_g. The E_g values (●) were established using the FKO intercept method. The solid line follows the relationship $E_g = 1.519 - 5.405 \times 10^{-4}[T^2/(T+204\ \mathrm{K})]$ eV due to Thurmond (Ref. 15).

The excitation energy of the traps appears to be affected by the coatings. The marked decrease in the trap-related PR in the $Al_xGa_{1-x}As$-coated substrates indicates that the thermal excitation energy for the impurities or traps is higher in the presence of the coating, probably because the coating produces an additional potential barrier to the removal of carriers from the interface region. Similarly, curves 6 and 7 of Fig. 8 show that the amplitude of structure *A* peaks at a lower temperature for substrates which were covered with doped GaAs epilayers in comparison with substrates covered by undoped epilayers. This shift also appears to be due to a change in the thermal excitation energy for the impurities or traps in presence of doped GaAs coating. The shift shown by curves 6 and 7 of Fig. 8, is about 5 meV, which corresponds to the energy of the Si impurity level in GaAs. This result is quite interesting because thermal excitation via Si impurities would imply that the mechanism for the trap-related PR involves electrons which are free to move along the interface. The process of excitation could thus involve two steps, a thermal dissociation along the interface and a thermal excitation out of the interface region. Initial attempts at detection of time-dependent PR showed no long-lifetime effects.

The modulation mechanism for PR from the epilayer-substrate interface appears to be related to the carrier mobility. The fact that the interface PR is observed through nearly 4 μm of GaAs indicates that the mechanism depends on the transport of laser-injected carriers. The absorption of the laser light occurs within the first 300 nm of the epilayer surface.[20] The electric field and its modulation at the interface of the undoped epilayer with the semi-insulating bulk should be negligible. Thus, the modulation mechanism for structure *A* could come from the thermal excitation of impurities or traps at the interface and their momentary refilling by the laser-injected carriers. This suggestion is further supported by the sharp increase in structure *A* with Hall mobility and epilayer doping. However, the overall increase in structure *A* with epilayer doping (see Fig. 10) could also be attributed to the lower light absorption by doped epilayers. In pure GaAs, the absorption peak at the exciton energy is generally quite prominent, but it is lowered by doping.[20]

Modulation through laser-induced changes in absorption of GaAs also appear to play a role in the amplitude of the PR from the interface. Structure *A* increases anomalously with the increase in laser intensity for undoped epilayers, Fig. 15. This behavior could be attributed to changes in absorption caused by laser-injected carriers, especially in the thin region of laser light absorption.[22,23] The laser-induced changes in absorption constitute an additional PR modulation mechanism, which could be responsible for the excitonic PR under low-field conditions in the undoped MBE samples and in the semi-insulating material. In doped epilayers, the exciton absorption peak is already reduced by doping[20,21] and the laser-injected carrier density can be neglected. Thus, for the doped epilayers, the behavior of structure *A* with laser intensity, Fig. 15, is the same as the behavior for the impurity PR from the bare substrate.

The PR from the traps or impurities has an inherent nature, and it is substantially higher than the PR from spurious contaminants which are sometimes observed in the 15–25-meV region below the band gap. Over 30 different samples have been examined in this study. The PR from the impurities or traps has been observed in all bulk samples and all thinly coated samples. The traps appear to be inherent to the semi-insulating surface. Thick MBE samples did not show a similar PR. Etching of the substrates did not change the energy or the amplitude of the trap-related PR.

ACKNOWLEDGMENTS

This research was sponsored by the U.S. Air Force Office of Scientific Research, Air Force Systems Command AFSC, United States Air Force, under Contract No. F49620-88-C-0053. We would like to give special thanks to Dr. D. K. Gaskill and Dr. W. M. Theis for helpful discussions and help with the samples and equipment. We would also like to thank B. Lampert, N. McDevitt, Dr. M. Donley, and D. Tomich for their technical assistance in MBE.

[1]W. Franz, Z. Naturforsch. **13a**, 484 (1958).
[2]L. V. Keldysh, Zh. Eksp. Teor. Fiz. **34**, 1138 (1958) [Sov. Phys.—JETP **7**, 788 (1958)].
[3]M. Cardona, *Modulation Spectroscopy* (Academic, New York, 1969).
[4]*Semiconductors and Semimetals,* edited by R. K. Willardson and A. C. Beer (Academic, New York, 1972), Vol. 9.
[5]J. L. Shay, Phys. Rev. B **2**, 803 (1970); J. L. Shay and R. E. Nahory, Solid State Commun. **7**, 945 (1969).
[6]D. E. Aspnes, Phys. Rev. B **10**, 4228 (1974); Surf. Sci. **37**, 418 (1973).
[7]D. E. Aspnes and A. A. Studna, Phys. Rev. B **7**, 4605 (1973).
[8]L. Peters, L. Phaneuf, L. W. Kapitan, and W. M. Theis, J. Appl. Phys. **62**, 4558 (1987).
[9]N. Bottka, D. K. Gaskill, R. S. Sillmon, R. Henry, and R. Glosser, J. Electron. Mater. **17**, 161 (1988).
[10]H. C. Casey and M. B. Panish, in *Heterostructure Lasers, Part B, Fundamental Principles* (Academic, New York, 1978).
[11]R. N. Bhattacharya, H. Shen, P. Parayanthal, Fred H. Pollak, T. Coutts, and H. Aharoni, Phys. Rev. B **37**, 4044 (1988).
[12]N. Bottka, D. K. Gaskill, R. J. M. Griffiths, R. R. Bradley, T. B. Joyce, C. Ito, and D. McIntyre, J. Crystal Growth **93**, 481 (1988).
[13]W. E. Spicer, I. Lindau, P. Skeath, C. Y. Su, and Patrick Chye, Phys. Rev. Lett. **44**, 420 (1980).
[14]M. Sydor, J. E. Angelo, T. W. Haas, W. Mitchel, and Ming-Yuan Yen, J. Appl. Phys. **66**, 156 (1989).
[15]C. D. Thurmond, J. Electrochem. Soc. **122**, 1133 (1975).

[16]W. M. Theis, G. D. Sanders, C. E. Leak, K. K. Bajaj, and H. Morkoç, Phys. Rev. B **37**, 3042 (1987).
[17]R. P. Silberstein and Fred H. Pollak, J. Vac. Sci. Technol. **17**, 1052 (1980).
[18]O. J. Glembocki, N. Bottka, and J. E. Furneaux, J. Appl. Phys. **57**, 432 (1985).
[19]D. Huang, G. Ji, U. K. Reddy, H. Morkoç, F. Xiong, and T. A. Tombrello, J. Appl. Phys. **63**, 5447 (1988).
[20]J. S. Blakemore, J. Appl. Phys. **53**, R123 (1982).
[21]J. G. Mendoza-Alvarez, F. D. Nunes, and N. B. Patel, J. Appl. Phys. **51**, 4365 (1980).
[22]D.A.B. Miller, D. S. Chemla, and S. Schmitt-Rink, Phys. Rev. B **33**, 6976 (1986).
[23]A. P. Thorn, A. J. Shields, P. C. Klipstein, N. Apsley, and T. M. Kerr, J. Phys. C **20**, 4229 (1987).